CLNS98/1598

hep-ph/9812442

Sixth-Order Vacuum-Polarization Contribution to the Lamb Shift of the Muonic Hydrogen

T. Kinoshita*

Newman Laboratory of Nuclear Studies, Cornell University, Ithaca, NY 14853

M. Nio†

Graduate School of Human Culture, Nara Women's University, Nara, Japan 630

Abstract

The sixth-order electron-loop vacuum-polarization contribution to the $2P_{1/2} - 2S_{1/2}$ Lamb shift of the muonic hydrogen ($\mu^- p^+$ bound state) has been evaluated numerically. Our result is 0.005295 (1) meV. This eliminates the largest uncertainty in the theoretical calculation. Combined with the proposed precision measurement of the Lamb shift it will lead to a very precise determination of the proton charge radius.

PACS numbers: 36.10.Dr, 12.20.Ds, 31.30.Jv, 06.20.Jr

Typeset using REVTEX

*e-mail: tk@hepth.cornell.edu

†e-mail: makiko@phys.nara-wu.ac.jp

The muonic hydrogen, the $\mu^- p^+$ bound state, differs from the ordinary hydrogen atom in two important respects. One is that the vacuum-polarization effect is much more important than other radiative corrections. The other is that it is more sensitive to the hadronic structure of the proton. Thus it provides a means of testing aspects of QED significantly different from those of the hydrogen atom.

Just as in the ordinary hydrogen atom, the muonic hydrogen has a long-lived 2S metastable state. This makes it possible to measure the $2P_{1/2} - 2S_{1/2}$ Lamb shift to about 10 ppm level using the phase-space compressed muon beam technique [1]. At present, however, theoretical precision of the Lamb shift is limited to the level of about 30 ppm. This uncertainty comes mainly from the unknown contribution $\Delta E^{(6)}$ of the sixth-order electron vacuum-polarization effect [2].

In this paper we report the result of our evaluation of $\Delta E^{(6)}$. Relevant integrals obtained using the exact sixth-order vacuum-polarization function [3] are summarized in Table I. Our result is

$$\begin{aligned} \Delta E^{(6)} &= 0.083\ 539\ (11)\ m_r (Z\alpha)^2 \left(\frac{\alpha}{\pi}\right)^3 \\ &= 0.005\ 295\ (1)\ \ \text{meV}, \end{aligned} \tag{1}$$

where $Z = 1$ for the proton and m_r is the reduced mass of the $\mu^- p^+$ system: [4]

$$\begin{aligned} m_r &= \frac{m_\mu m_p}{m_\mu + m_p} = 94.964\ 485\ (28)\ \text{MeV}, \\ m_\mu &= 105.658\ 389(34)\ \ \text{MeV}, \\ m_p &= 938.272\ 31(28)\ \ \text{MeV}\ \ . \end{aligned} \tag{2}$$

We have also evaluated the main part of $\Delta E^{(6)}$ using the Padé approximation of vacuum-polarization function [5]. The result (23) of this calculation is in good agreement with the direct calculation (22). A more detailed comparison of these results will be given in a separate paper [6].

The vacuum-polarization contribution to the $2P_{1/2} - 2S_{1/2}$ Lamb Shift of the muonic hydrogen can be expressed as an integral over the vacuum-polarization function $\Pi(q^2)$. Here

q may be either space-like or time-like. The first choice ($q^2 < 0$) leads to the integral

$$\Delta^{(I)}E = \int \frac{d^3q}{(2\pi)^3}\tilde{\rho}(a^2)\frac{-4\pi Z\alpha}{\vec{q}^2}\left[-\Pi(-\vec{q}^2)\right]$$
$$= \frac{2}{\pi}(Z\alpha)^2 m_r \int_0^\infty da\tilde{\rho}(a^2)\Pi(-(Z\alpha m_r)^2 a^2). \tag{3}$$

The function $\tilde{\rho}$ is equal to $\tilde{\rho}_{2P} - \tilde{\rho}_{2S}$, where $\tilde{\rho}_{2P}$ and $\tilde{\rho}_{2S}$ are Fourier transforms of the squares of non-relativistic Coulomb wave functions for the $2P$ and $2S$ states, respectively:

$$\tilde{\rho}_{2P(2S)} = \int d^3r |\phi_{2P(2S)}(\vec{r})|^2 e^{-i\vec{p}\cdot\vec{r}}. \tag{4}$$

For the $2P$ states, we take the average over three degenerate states. Carrying out this integration we obtain

$$\tilde{\rho}_{2P} = \frac{1-a^2}{(1+a^2)^4}\ , \qquad \tilde{\rho}_{2S} = \frac{1-3a^2+2a^4}{(1+a^2)^4}\ , \tag{5}$$

where $a = |\vec{p}|/(Z\alpha m_r)$.

The second choice ($q^2 > 0$) gives rise to the integral [2]

$$\Delta^{(II)}E = m_r(Z\alpha)^2 \int_4^\infty dt u(t)\frac{\beta^2}{2(1+\beta\sqrt{t})^4}\ , \tag{6}$$

where

$$\beta = \frac{m_e}{m_r\alpha} = 0.737\ 383\ 76\ (30) \tag{7}$$

and $u(t)$ is the imaginary part of the vacuum-polarization function $\Pi(q^2)$

$$u(t) = \frac{1}{\pi} Im\Pi(q^2 = tm_e^2)\ \ . \tag{8}$$

Although Eqs. (3) and (6) are analytically equivalent, they are totally different from the viewpoint of numerical integration. Thus they provide a useful check whenever both real and imaginary parts of Π are available. For diagrams containing several vacuum-polarization loops in one Coulomb photon line, Eqs. (3) and (6) must be modified accordingly.

Let us first consider the contribution coming from three second-order vacuum-polarization insertions in a Coulomb photon (see Fig. 1). The contribution $\Pi^{(p2:3)}(q^2)$ of

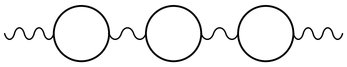

FIG. 1. Three second-order vacuum-polarization diagrams inserted in the Coulomb photon line exchanged by the muon and the proton.

this improper diagram can be expressed in terms of the second-order vacuum-polarization function $\Pi^{(2)}(q^2)$ as

$$\Pi^{(p2:3)}(q^2) = (\Pi^{(2)}(q^2))^3 \ , \tag{9}$$

where $\Pi^{(2)}$ is known analytically and has the spectral function

$$u^{(2)}(t) = \frac{1}{3}\frac{\alpha}{\pi}\sqrt{1-\frac{4m_e^2}{q^2}}\left(1+\frac{2m_e^2}{q^2}\right), \quad q^2 \geq 4m_e^2. \tag{10}$$

Substituting $\Pi^{(p2:3)}$ in Eq. (3) and evaluating the integral numerically,[1] we find

$$\begin{aligned}\Delta^{(I)}E^{(p2:3)} &= 0.006\ 253\ 4\ (6)\ m_r(Z\alpha)^2\left(\frac{\alpha}{\pi}\right)^3 \\ &= 0.000\ 396\ 33\ (4)\ \text{meV}\ .\end{aligned} \tag{11}$$

The result of the second method based on Eq. (6) is in good agreement with (11):

$$\begin{aligned}\Delta^{(II)}E^{(p2:3)} &= 0.006\ 253\ 9\ (10)\ m_r(Z\alpha)^2\left(\frac{\alpha}{\pi}\right)^3 \\ &= 0.000\ 396\ 36\ (6)\ \text{meV}\ .\end{aligned} \tag{12}$$

The quantity $\Delta^{(I)}E^{(p2:3)}$ can also be evaluated using the parametric-integral form of $\Pi^{(2)}$ given in Ref. [3]. This leads to

$$\begin{aligned}\Delta^{(I)}E^{(p2:3)} &= 0.006\ 253\ 8\ (8)\ m_r(Z\alpha)^2\left(\frac{\alpha}{\pi}\right)^3 \\ &= 0.000\ 396\ 35\ (5)\ \text{meV}\ .\end{aligned} \tag{13}$$

The next contribution comes from diagrams involving one second-order and one fourth-order vacuum-polarization insertions (see Fig. 2). This contribution is given in terms of

[1]This and subsequent integrals are evaluated numerically on DECα by the adaptive-iterative Monte-Carlo subroutine VEGAS [7].

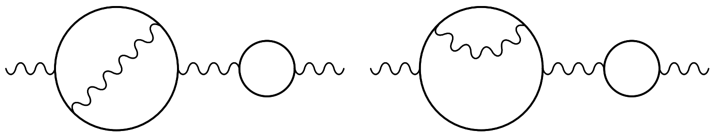

FIG. 2. Insertion of one second- and one fourth-order vacuum-polarization diagrams in the Coulomb photon line exchanged by the muon and the proton.

$$\Pi^{(p4p2)}(q^2) = -2\Pi^{(2)}(q^2)\Pi^{(4)}(q^2) \ , \tag{14}$$

where $\Pi^{(4)}$ is the fourth-order vacuum-polarization function. Substituting $\Pi^{(4)}$ derived from Ref. [8] into Eq. (3) we obtain

$$\begin{aligned} \Delta^{(I)}E^{(p4p2)} &= 0.046\ 248\ (5)\ m_r(Z\alpha)^2\left(\frac{\alpha}{\pi}\right)^3 \\ &= 0.002\ 931\ (1)\ \text{meV} \ , \end{aligned} \tag{15}$$

while Eq. (6) leads to

$$\begin{aligned} \Delta^{(II)}E^{(p4p2)} &= 0.046\ 243\ (16)\ m_r(Z\alpha)^2\left(\frac{\alpha}{\pi}\right)^3 \\ &= 0.002\ 931\ (2)\ \text{meV} \ . \end{aligned} \tag{16}$$

We have also evaluated $\Delta^{(I)}E^{(p4p2)}$ using the parametric-integral form of $\Pi^{(4)}$ [3]:

$$\begin{aligned} \Delta^{(I)}E^{(p4p2)} &= 0.046\ 250\ (2)\ m_r(Z\alpha)^2\left(\frac{\alpha}{\pi}\right)^3 \\ &= 0.002\ 931\ (1)\ \text{meV} \ . \end{aligned} \tag{17}$$

No convenient parametric integral is available for the second method.

The third contribution comes from the sixth-order vacuum-polarization term $\Pi^{(p4(p2))}$ obtained by inserting a second-order vacuum-polarization loop in the fourth-order vacuum-polarization diagram (see Fig. 3). The form of $\Pi^{(p4(p2))}$ convenient for numerical integration is as integral over Feynman parameters [3]. A useful form of the imaginary part of $\Pi^{(p4(p2))}$ is not available. (It is true that it can be written formally as an integral involving a δ-function. But this is not convenient for numerical integration.) Thus we use Eq. (3) only. This can be done easily by adapting to the Lamb shift the program written previously for the electron $g-2$ involving vacuum polarization insertion [9]. This leads to

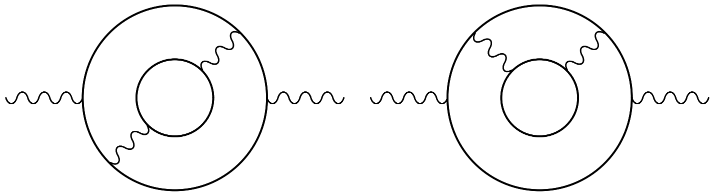

FIG. 3. Sixth-order vacuum-polarization diagrams with a second-order vacuum-polarization inserted in the fourth-order vacuum-polarization diagrams.

$$\begin{aligned}\Delta^{(I)} E^{(p4(p2))} &= 0.013\ 628\ (6)\ m_r (Z\alpha)^2 \left(\frac{\alpha}{\pi}\right)^3 \\ &= 0.000\ 864\ (1)\ \text{meV}\ .\end{aligned} \tag{18}$$

The last and most complicated contribution comes from the sixth-order vacuum-polarization diagrams with a single electron loop. The exact form of this contribution is known only in a parametric-integral form [3]. Its imaginary part is not available in a form convenient for numerical integration. We have therefore evaluated it using Eq. (3) only. There are eight topologically distinct diagrams (see Fig. 4). Each diagram can be written as a sum of various divergent terms and a finite part $\Delta\Pi^{(6i)}$, where $i = a, b, ..., h$. After renormalization the sum of these diagrams is free from any divergence and can be written as [3]

$$\begin{aligned}\Pi^{(p6)} &= 2(\Delta\Pi^{(6a)} + \Delta\Pi^{(6c)} + \Delta\Pi^{(6d)} + \Delta\Pi^{(6f)}) \\ &\quad + \Delta\Pi^{(6b)} + 4\Delta\Pi^{(6e)} + \Delta\Pi^{(6g)} + \Delta\Pi^{(6h)} - 4\Delta B_2 \Pi^{(4)} \\ &\quad - 2[\Delta B_{4a} + \Delta L_{4x} + 2\Delta L_{4c} + \Delta B_{4b} + \Delta L_{4l} + 2\Delta L_{4s} + \frac{3}{2}(\Delta B_2)^2]\Pi^{(2)} \\ &\quad - 2(\Delta\delta m_{4a} + \Delta\delta m_{4b})\Pi^{(2*)}\ ,\end{aligned} \tag{19}$$

where $\Delta B_2,\ \cdots$, are finite parts of renormalization constants free from ultraviolet- and infrared-divergences and $\Pi^{(2)}$ and $\Pi^{(4)}$ are renormalized vacuum-polarization functions of second- and fourth-order, respectively. $\Pi^{(2*)}$ is the second-order vacuum-polarization function with a mass insertion vertex. Precise definitions of these functions are given in Ref. [10]. The numerical values of the coefficients of $\Pi^{(4)}$, $\Pi^{(2)}$ and $\Pi^{(2*)}$ are

$$\Delta B_2 = \frac{3}{4}\,\frac{\alpha}{\pi}\ ,$$

$$\Delta B_{4a} + \ \cdots \ + \frac{3}{2}(\Delta B_2)^2 = 0.871\ 680\ (27)\Big(\frac{\alpha}{\pi}\Big)^2,$$
$$\Delta\delta m_{4a} + \Delta\delta m_{4b} = 1.906\ 340\ (21)\Big(\frac{\alpha}{\pi}\Big)^2\ , \tag{20}$$

where the last two are new evaluations. The Lamb Shift contributions from $\Pi^{(4)}$, $\Pi^{(2)}$, and $\Pi^{(2*)}$ can be easily obtained by numerical integration:

$$\begin{aligned}\Delta E^{(p4)} &= 0.045\ 922\ 7\ (4)\ m_r(Z\alpha)^2\Big(\frac{\alpha}{\pi}\Big)^2\ ,\\ \Delta E^{(p2)} &= 0.017\ 452\ 8\ (3)\ m_r(Z\alpha)^2\frac{\alpha}{\pi}\ ,\\ \Delta E^{(p2*)} &= -0.009\ 001\ 8\ (2)\ m_r(Z\alpha)^2\frac{\alpha}{\pi}.\end{aligned} \tag{21}$$

The Lamb Shift contributions $\Delta E^{(p6a)}, \cdots$, coming from the ultraviolet- and infrared-finite parts of diagrams $\Delta\Pi^{(6a)}, \cdots$, are numerically evaluated. The results are summarized in Table II. The second and third columns list the results of integration carried out in double precision[2] and quadruple precision, respectively. The former integration uses 100 million sampling points per iteration while the latter uses 1 million sampling points per iteration (except for the diagrams $6a$ and $6e$ which use 2 and 4 times more sampling points, respectively). The number of iteration is 50. The purpose of the latter calculation is to see whether the former indicates sign of losing significant digits due to rounding-off, which is the major source of uncertainty of this type of calculation. Column 4 gives the difference between columns 2 and 3. The excellent agreement between two calculations shows that the estimated error of the former is not significantly affected by rounding-off and can be safely assumed to be mostly statistical. We therefore choose the double precision value, which has higher statistics, as our best estimate:

$$\begin{aligned}\Delta^{(I)}E^{(p6)} &= 0.017\ 410\ (9)\ m_r(Z\alpha)^2\ \Big(\frac{\alpha}{\pi}\Big)^3\\ &= 0.001\ 103\ (1)\ \text{meV}\ .\end{aligned} \tag{22}$$

[2]The double precision calculation is carried out on Fujitsu-VX of Computer Center, Nara Women's University.

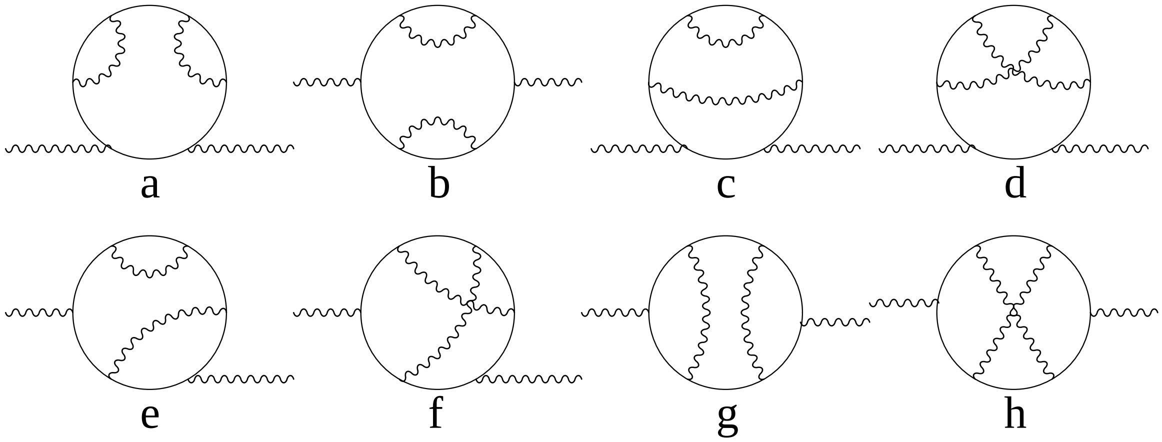

FIG. 4. Sixth-order vacuum-polarization diagrams with a single electron loop.

As a cross-check, we have also evaluated $\Delta E^{(p6)}$ using the Padé-approximation of the vacuum-polarization function given in Ref. [5]. We have done this using both methods I and II. The [2/3] and [3/2] Padé approximations give nearly identical results. Taking their average we obtain

$$\begin{aligned}\Delta^{(I)} E^{(p6)}_{Padé} &= 0.017\ 414\ 9\ (25)\ m_r (Z\alpha)^2 \left(\frac{\alpha}{\pi}\right)^3 , \\ \Delta^{(II)} E^{(p6)}_{Padé} &= 0.017\ 414\ 9\ (26)\ m_r (Z\alpha)^2 \left(\frac{\alpha}{\pi}\right)^3 . \end{aligned} \tag{23}$$

These results are consistent with each other and agree with (22) in the first three significant digits, or within one standard deviation of (22). Obviously either (22) or (23) has sufficient precision as far as comparison with experiment is concerned. Note, however, that the uncertainties given in (23) are those resulting from numerical treatment of the Padé approximation and do not include those caused by the Padé method itself. It is argued in a separate paper [6], however, that the uncertainty of the Padé model itself is about 0.001 percent and hence the true value will be found well within the uncertainties quoted in (23).

Collecting (11), (15), (18), and (22), we find the total contribution to the Lamb Shift due to the sixth-order vacuum-polarization insertion in a Coulomb photon line to be

$$\begin{aligned}\Delta E^{(6)} &= \Delta E^{(p2:3)} + \Delta E^{(p4p2)} + \Delta E^{(p4(p2))} + \Delta E^{(p6)} \\ &= 0.083\ 539\ (11)\ m_r \alpha^2 \left(\frac{\alpha}{\pi}\right)^3 \end{aligned}$$

$$= 0.005\ 295\ (1)\ \text{meV}\ . \tag{24}$$

Evaluation of various lower-order contributions to the $2P_{1/2} - 2S_{1/2}$ Lamb shift $\mathcal{L}$ of the muonic hydrogen are summarized in Ref. [2]. Inclusion of our result (24) leads to a much more precise theoretical prediction

$$\mathcal{L} = (205.937\ (1) - 5.197\ 5\ r_p^2)\ \text{meV}, \tag{25}$$

where r_p is the proton charge radius in units of fm. The remaining uncertainty in the first term of (25) will be at most of the order of 0.001 meV [11]. Although this estimate is sufficient for the precision of the forthcoming measurement, more precise estimate may be needed in the future. Measurement of $\mathcal{L}$ to 10 ppm, or 0.002 meV, will lead to improvement in the value of r_p^2 by a factor of 50 over those determined from the elastic scattering form factor measurements, making it possible to resolve the long-standing discrepancy between [12] and [13]. The new value of r_p^2 will also play an important role in testing the validity of QED in terms of high precision measurements of the spectrum of the hydrogen atom [14]. Another impact of accurate determination of r_p^2 will be to stimulate evaluation of r_p^2 from the lattice QCD more precise and reliable than those available at present [15].

ACKNOWLEDGMENTS

We should like to thank D. Taqqu for communicating about the proposed measurement of the Lamb shift of the muonic hydrogen. The work of T. K. is supported in part by the U. S. National Science Foundation. The work of M. N. is supported in part by the Grant-in-Aid (No. 10740123) of the Ministry of Education, Science, and Culture, Japan. Part of numerical calculations was carried out on Fujitsu-VX of Computer Center, Nara Women's University.

REFERENCES

[1] D. Taqqu *et al.*, Hyp. Int. **101/102**, 599 (1996).

[2] K. Pachucki, Phys. Rev. A **53**, 2092 (1996).

[3] T. Kinoshita and W. B. Lindquist, Phys. Rev. D **27**, 853 (1983).

[4] C. Caso *et al.*, Euro. Phys. J. **C3**, 1 (1998).

[5] P. A. Baikov and D. J. Broadhurst, in *New Computing Techniques in Physics Research IV*, eds. B. Denby and D. Perret-Gallix (World Scientific, Singapore, 1995), pp. 167 -172.

[6] T. Kinoshita and M. Nio, CLNS98/1599 and hep-ph/9812443.

[7] G. P. Lepage, J. Comput. Phys. **27**, 192 (1978).

[8] G. Källén and A. Sabry, K. Dan. Vidensk. Selsk. Mat.-Fys. Medd. **29**, No. 17 (1955).

[9] T. Kinoshita and W. B. Lindquist, Phys. Rev. D **27**, 867 (1983).

[10] P. Cvitanović and T. Kinoshita, Phys. Rev. D **10**, 4007 (1974).

[11] K. Pachucki, private communication.

[12] G. G. Simon, C. Schmidt, F. Borkowski, and V. H. Walther, Nucl. Phys. A **333**, 381 (1980).

[13] L. N. Hand, D. J. Miller, and R. Wilson, Rev. Mod. Phys. **35**, 335 (1963).

[14] Th. Udem *et al.*, Phys. Rev. Lett. **79**, 2646 (1997).

[15] T. Drapers, R. M. Woloshin, and K.-F. Liu, Phys. Lett. B **234**, 121 (1990); D. B. Leinweber and T. D. Cohen, Phys. Rev. D **47**, 2147 (1993).

TABLE I. Contribution to the $2P_{1/2}-2S_{1/2}$ muonic hydrogen Lamb shift from the sixth-order vacuum polarization diagrams of various types. The values (I) and (II) are obtained using Eqs. (3) and (6), respectively. The last two lines are in quadruple and double precision, respectively. The overall factor $m_r(Z\alpha)^2(\alpha/\pi)^3$ is omitted.

Term	Value (I)	Equation	Value (II)	Equation
$\Delta E^{(p2:3)}$	0.006 253 (1)	(11)	0.006 254 (1)	(12)
$\Delta E^{(p4p2)}$	0.046 248 (5)	(15)	0.046 242 (18)	(16)
$\Delta E^{(p4(p2))}$	0.013 628 (6)	(18)	not available	—
$\Delta E^{(p6)}_{\text{quad.}}$	0.017 354 (94)	(22)	not available	—
$\Delta E^{(p6)}_{\text{double}}$	0.017 410 (9)	(22)	not available	—

TABLE II. Contributions to the $2P_{1/2}-2S_{1/2}$ muonic hydrogen Lamb shift from the sixth-order vacuum polarization diagrams with a single electron loop. The overall factor $m_r(Z\alpha)^2(\alpha/\pi)^3$ is omitted. The second and third columns give results of integration in double precision and quadruple precision, respectively. Their difference is listed in column 4.

Term	Double precision	Quad. precision	Difference
$\Delta E^{(6a)}$	0.044 769 (4)	0.044 739 (51)	0.000 030 (52)
$\Delta E^{(6b)}$	0.028 654 (4)	0.028 640 (35)	0.000 014 (36)
$\Delta E^{(6c)}$	−0.025 393 (3)	−0.025 368 (23)	−0.000 025 (24)
$\Delta E^{(6d)}$	−0.026 376 (2)	−0.026 371 (21)	−0.000 005 (22)
$\Delta E^{(6e)}$	0.151 356 (4)	0.151 334 (46)	0.000 022 (47)
$\Delta E^{(6f)}$	−0.067 139 (3)	−0.067 144 (30)	0.000 005 (31)
$\Delta E^{(6g)}$	0.019 536 (3)	0.019 540 (23)	−0.000 004 (24)
$\Delta E^{(6h)}$	0.025 877 (2)	0.025 858 (22)	0.000 019 (23)